High-resolution microPET imaging of carcinoembryonic antigen-positive xenografts by using a copper-64-labeled engineered antibody fragment

Anna M. Wu*†‡, Paul J. Yazaki*, Shih-wa Tsai*, Khoi Nguyen‡, Anne-Line Anderson§, Deborah W. McCarthy¶, Michael J. Welch¶, John E. Shively*, Lawrence E. Williams§, Andrew A. Raubitschek§, Jeffrey Y. C. Wong§, Tatsushi Toyokuni‡, Michael E. Phelps‡, and Sanjiv S. Gambhir†‡

*Beckman Research Institute of the City of Hope, Duarte, CA 91010; ‡Department of Molecular and Medical Pharmacology, Crump Institute for Biological Imaging, University of California School of Medicine, Los Angeles, CA 90095; §City of Hope National Medical Center, Duarte, CA 91010; and ¶Mallinckrodt Institute of Radiology, Washington University Medical School, St. Louis, MO 63110

Contributed by Michael E. Phelps, May 19, 2000

Rapid imaging by antitumor antibodies has been limited by the prolonged targeting kinetics and clearance of labeled whole antibodies. Genetically engineered fragments with rapid access and high retention in tumor tissue combined with rapid blood clearance are suitable for labeling with short-lived radionuclides, including positron-emitting isotopes for positron-emission tomography (PET). An engineered fragment was developed from the high-affinity anticarcinoembryonic antigen (CEA) monoclonal antibody T84.66. This single-chain variable fragment (Fv)-C_H3, or minibody, was produced as a bivalent 80 kDa dimer. The macrocyclic chelating agent 1,4,7,10-tetraazacyclododecane-*N,N′,N″,N‴*-tetraacetic acid (DOTA) was conjugated to the anti-CEA minibody for labeling with copper-64, a positron-emitting radionuclide ($t_{1/2}$ = 12.7 h). *In vivo* distribution was evaluated in athymic mice bearing paired LS174T human colon carcinoma (CEA positive) and C6 rat glioma (CEA negative) xenografts. Five hours after injection with ^{64}Cu-DOTA-minibody, microPET imaging showed high uptake in CEA-positive tumor (17.9% injected dose per gram ± 3.79) compared with control tumor (6.0% injected dose per gram ± 1.0). In addition, significant uptake was seen in liver, with low uptake in other tissues. Average target/background ratios relative to neighboring tissue were 3–4:1. Engineered antibody fragments labeled with positron-emitting isotopes such as copper-64 provide a new class of agents for PET imaging of tumors.

The diagnostic potential of radiolabeled antibodies that localize specifically to human malignancies is steadily being realized (1–3). However, currently available whole antibodies and fragments suffer from shortcomings as radiolabeled pharmaceuticals, including the prolonged biological half life of intact antibodies, leading to high background signal. Enzymatically derived fragments such as $F(ab')_2$ and Fab′, labeled with radioiodine, show more favorable targeting and clearance kinetics than whole immunoglobulins (4) and result in higher sensitivity at earlier times but are more tedious to produce. In addition, radiometal-labeled fragments, e.g., ^{99m}Tc-$F(ab')_2$ or Fab′, demonstrate increased renal activity (5), and targeting by Fab′ fragments may be inherently limited by their monovalent binding to antigen. Nonetheless, radioimmunoscintigraphy is playing an increasingly important role in the clinic (3).

A promising approach has been to genetically engineer antibody fragments to have appropriate properties for high targeted localization of a labeled fragment to a specific antigen, with low nontarget binding and rapid clearance from nonspecific sites *in vivo*. For example, by using the carcinoembryonic antigen (CEA) system, a series of engineered fragments was derived from the parental murine monoclonal antibody T84.66, selected for its high affinity and specificity for CEA (6). CEA is a well-established tumor-associated antigen, highly expressed in colorectal carcinoma and frequently elevated in adenocarcinomas of the lung, breast, other gastrointestinal organs, and ovary. Because expression in normal tissues is limited, CEA has proved to be a suitable target for antibody-based localization strategies (7–9). Single-chain Fv fragments (scFvs; constructed by assembling light and heavy chain variable regions with an engineered connecting peptide), diabodies (dimers of scFv), and an engineered fragment called the minibody (an scFv-C_H3 fusion protein) (Fig. 1) have been constructed from T84.66 and evaluated *in vivo* by using the athymic mouse/LS174T human colorectal carcinoma xenograft model (10–12). Results by using radioiodinated fragments showed that all three forms cleared rapidly from the bloodstream and that higher tumor uptakes were achieved as one progressed to the higher molecular weight bivalent fragments. In particular, the minibody format demonstrated a promising combination of rapid high-level accumulation of activity in xenografts and rapid disappearance from the circulation and many nontarget tissues. When minibody was radiolabeled with ^{123}I, a pure γ emitter with a 13.2 h half life, images that localized the xenograft could be acquired within 4 h of administration by using a standard γ camera (12). Preliminary biodistribution studies of ^{111}In-labeled minibodies demonstrated that they retain excellent localization to tumors and rapid blood clearance (P.J.Y., A.M.W., S.-W.T., L.E.W., D. N. Ikle, J.Y.C.W., J.E.S., and A.A.R., unpublished work).

Positron-emission tomography (PET) provides a high image contrast and quantitative method for detecting the location(s) and levels of radiotracer accumulation. Spatial resolution of current clinical PET scanners is ≈4–6 mm, whereas γ cameras are limited to a resolution of ≈12–15 mm. Furthermore, the sensitivity of PET is approximately 10-fold greater than that of single-photon techniques, allowing for more accurate detection of lower levels of radioactive tracer. PET has recently gained clinical acceptance in the staging and management of malignancies including lung, colorectal, melanoma, and lymphoma by using the tracer 2-deoxy-2-[^{18}F]fluoro-D-glucose (FDG) (re-

Abbreviations: PET, positron emission tomography; CEA, carcinoembryonic antigen; DOTA, 1,4,7,10-tetraazacyclododecane-*N,N′,N″,N‴*-tetraacetic acid; FDG, 2-deoxy-2-[^{18}F]fluoro-D-glucose; DWBA, digital whole body autoradiography; ROI, region of interest; %ID/g, percent injected dose per gram.

†To whom reprint requests should be addressed. E-mail: awu@coh.org or sgambhir@mednet.ucla.edu.

The publication costs of this article were defrayed in part by page charge payment. This article must therefore be hereby marked "*advertisement*" in accordance with 18 U.S.C. §1734 solely to indicate this fact.

Article published online before print: *Proc. Natl. Acad. Sci. USA*, 10.1073/pnas.150228297. Article and publication date are at www.pnas.org/cgi/doi/10.1073/pnas.150228297

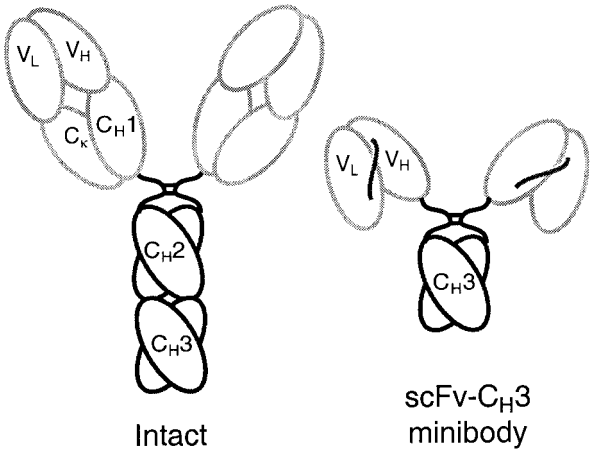

Fig. 1. Schematic overview of anti-CEA minibody. A gene encoding the minibody is assembled in the order V_L-linker-V_H-hinge-C_H3, with the hinge and C_H3 domains derived from human IgG1. The protein self assembles into 80-kDa dimers.

viewed in ref. 13). The increasing availability and lower cost of PET scanners and commercial PET radiopharmaceuticals allow routine imaging with PET in the care of cancer patients as well as provide the impetus to develop molecular imaging probes that are more specific for various cancers, to add to improved clinical management provided with FDG. To facilitate the testing of new positron-labeled agents in small-animal models, microPET technology has been developed that currently provides ($\approx$1.8 mm)^3 volumetric resolution (14). The microPET scanner has an axial field-of-view of 1.8 cm, and an entire mouse can be scanned by using multiple bed positions (14). Fully three-dimensional collection of emission data along with algebraic reconstruction techniques (15) lead to high-definition images of the whole body of the mouse.

Several laboratories have explored labeling of antibodies and fragments with positron-emitting isotopes for applications in cardiology and oncology. Long to intermediate half-life positron emitters such as iodine-124 ($t_{1/2}$ = 4.2 d), copper-64 ($t_{1/2}$ = 12.7 h) and fluorine-18 ($t_{1/2}$ = 110 min) are especially appealing for labeling antibodies. Targeting and imaging of ^{124}I-labeled whole antibodies have been evaluated preclinically in animal models of breast or ovarian cancer by using clinical PET scanners (16, 17). Extension of work to clinical studies demonstrated the potential of this approach to quantitative imaging and dose estimation for radioimmunotherapy trials (18, 19). However, the shortcomings of using whole antibodies, specifically their prolonged blood pool activity, remain apparent. Copper-64-labeled antibodies and fragments for lymphoma and colorectal cancer have been studied in animals and humans (20–23). Although target has been visualized and radioimmunotherapy in animals achieved (24), slow kinetics of target tissue uptake and blood and nonspecific tissue clearance remain an issue. Currently, fluorine-18 is the most widely used PET radioisotope; however, its short half life of less than 2 h demands rapid localization and clearance by tumor-specific antibodies. This can be achieved by use of ^{18}F-labeled Fab fragments (25, 26), disulfide-stabilized Fv (27), or potentially diabodies (11).

In the present work, we sought to evaluate the combination of an engineered antibody fragment (the anti-CEA minibody) having moderately rapid targeting with high rates of blood and tissue clearance *in vivo*, labeled with a positron-emitting radionuclide, copper-64, of intermediate half life (12.7 h). Furthermore, use of the microPET scanner offered the opportunity to evaluate targeting, biodistribution, and clearance in a living small-animal model of disease with very high resolution and sensitivity.

Methods

Production, Purification, and Conjugation of the T84.66 GS18 Minibody. The anti-CEA scFv-C_H3 fusion protein used in these studies was based on previously published work (12) except for the use of a longer (18-aa) linker between the variable domains (GS18 linker). The T84.66/GS18 minibody was expressed in NS0 murine myeloma cells by using the pEE12 expression vector with a cytomegalovirus promotor and glutamine synthetase as the selectable marker (Lonza Biologics, Slough, Berkshire, U.K.) (28, 29). Protein was purified by hydrophobic interaction chromatography (Source ISO, Amersham Pharmacia Biotech) followed by anion exchange chromatography (HQ50, Perkin–Elmer) by using a Perkin–Elmer BioCAD 700E perfusion chromatography system. Activity was determined by ELISA by using microtiter wells coated with a recombinant CEA protein (N and A3 domains) (30) and anti-human Fc (Jackson ImmunoResearch) for detection.

Purified T84.66/GS18 minibody was conjugated to 1,4,7,10-tetraazacyclododecane-*N,N′,N″,N‴*-tetraacetic acid (DOTA) by using the water-soluble *N*-hydroxysuccinimide method of Lewis *et al.* (31). Typically, 2 mg of protein was reacted with a 1,000:1 ratio of DOTA to protein for 18–24 h at 4°C at pH 7.0. After conjugation, the protein was dialyzed extensively in 0.2 M NH_4OAc, pH 7.2, and concentrated to greater than 5 mg/ml. The DOTA/antibody conjugation ratio was determined by incubation of the DOTA-conjugated minibody with a labeling solution containing known quantities of ^{111}In (Mallinckrodt) and cold indium (Aldrich). Labeling was analyzed by instant TLC by using Monoclonal Antibody ITLC strips (Biodex Medical Systems, Shirley, NY). Percent bound indium was determined and the DOTA/antibody ratios calculated.

Copper-64 Radiolabeling of GS18 Minibody. Copper-64 (copper chloride in 0.1 M HCl; radionuclide purity >99%) was produced in a cyclotron from enriched ^{64}Ni targets at the Mallinckrodt Institute of Radiology (32, 33). DOTA-conjugated minibody (200 μg) was incubated with 1.5 mCi of ^{64}Cu in 0.1 M NH_4 citrate, pH 5.5, for 1 h at 43°C. The reaction was terminated by addition of EDTA to 1 mM. Labeled protein was purified by size-exclusion HPLC on a TSK2000 column (30 cm $\times$ 7.5 mm i.d.; TosoHaas, Montgomeryville, PA). Radiolabeling efficiency was determined by integrating areas on the HPLC trace and determining the percentage of radioactivity associated with the 80-kDa protein peak. Immunoreactivity was determined by incubation of the labeled protein with a 20-fold excess (wt/wt) of either purified CEA or the recombinant N-A3 fragment of CEA in 0.15 ml of PBS/1% HSA. Samples were analyzed by size-exclusion HPLC to assess formation of Ab/Ag complexes, and peak heights were integrated.

Cell Lines and Xenografts. All animal handling was performed in accordance with University of California, Los Angeles (UCLA), Animal Research Committee guidelines. The LS174T human colorectal carcinoma cell line (CL 188) and C6 rat glioma cell line (CCL 107) were obtained from American Type Culture Collection and maintained under standard conditions. Xenografts were established in 7-week-old female CD1 nude mice (Charles River Breeding Laboratories) by s.c. inoculation of 1–2 $\times$ 10^6 cells 10–14 days before imaging studies. In some experiments, after scanning, tumors were excised, weighed, and counted in a well counter (Cobra II AutoGamma, Packard, IL).

For some mice, tumor, liver, and kidney tissues were excised, fixed in buffered formalin, and embedded in paraffin for immunohistochemical analysis. Five-micrometer sections were cut and mounted, deparaffinized, and rehydrated, and antigen re-

trieval was achieved by steaming with 0.01 M EDTA·Tris, pH 8.0, for 20 min (34). Sections were stained by using chimeric T84.66 anti-CEA antibody and developed by using a modified avidin–biotin complex method (Vantana Medical System, Tucson, AZ) according to the manufacturer's instructions.

MicroPET Scanning. Mice were imaged by using the microPET scanner developed at the Crump Institute for Biological Imaging (UCLA), also available through Concorde Microsystems (Knoxville, TN). Mice were injected in the tail vein with 26–88 μCi of ^{64}Cu-minibody (specific activity, 3.4–5.5 μCi/μg at the time of radiolabeling). After the appropriate time had elapsed, mice were anesthetized with ketamine 100 mg/kg, xylazine 7 mg/kg, injected i.p., placed in a prone position, and imaged by using the microPET scanner with the long axis of the mouse parallel to the long axis of the scanner. Acquisition time was 56 min (8 min per bed position; 7 bed positions), and images were reconstructed by using a MAP reconstruction algorithm (15). Some mice were also imaged by using FDG a day or two before the ^{64}Cu-minibody scan. Mice were administered 150–200 μCi of FDG via the tail vein, and scans were acquired as described above, beginning 1 h after tracer injection.

Digital Whole-Body Autoradiography (DWBA). Mice were killed and frozen in 4% carboxymethyl-cellulose (Aldrich) in preparation for sectioning with a PMV cryostat (Stockholm, Sweden). Coronal cross sections were obtained with a thickness of 45 μm. Anatomical digital photographs of each coronal section were also obtained. DWBA were obtained by using a Fuji BAS 5000 Phosphorimager and digital plates with a final resolution of $\approx$100 μm (35). All DWBA were analyzed by using MAC BAS software version 2.4 (Fuji).

Data Analysis. Quantitation of microPET images was performed by using the Crump Institute Integrated Imaging Software Package (CRIIISP). Regions of interest (ROIs) were drawn for both the control and LS174T CEA-positive tumors centered on the peak of the activity profile. ROI counts/pixel/min were converted to counts/cc/min by using a calibration factor obtained from scanning a cylinder containing copper-64. These data were converted to percent injected dose per gram (%ID/g) by dividing by the count rate of the injected activity. ROIs were also drawn over adjacent shoulder regions for measurement of soft-tissue activity (primarily muscle). The effects of ROI positioning were determined by averaging at least four ROIs and assessing the variability across regions. ROIs were also drawn on DWBA images and quantitated by using MAC BAS software. All statistical analysis was performed by using Excel. A student's *t* test was used to test the hypothesis that there are significant differences in the %ID/g tumor between the control and LS174T tumors.

Results

Rapid Labeling of Anti-CEA Minibody with ^{64}Cu Yielded a Tracer with High Specific Activity and Immunoreactivity. Preparation of DOTA-conjugated T84.66/GS18 minibody provided a means for labeling the protein with a variety of radiometals, including copper-64. The chelate/antibody ratios, determined by incubation of the protein with various known concentrations of carrier-added ^{111}In, ranged from 5:1 to 6:1 for DOTA/minibody. A 1-h labeling time at 43°C proved sufficient for 80–90% incorporation of ^{64}Cu into the protein (Fig. 2*A*), and the entire procedure, including HPLC purification, required 2 h. Specific activities after labeling (n = 5) ranged from 3.4–5.5 μCi/μg (272–400 Ci/mmol of 80-kDa protein). As shown in Fig. 2*B*, the radiolabeled minibody retained high immunoreactivity against CEA; in this experiment, peak integration demonstrated that 95% of the radioactivity was shifted into higher molecular weight complexes after incubation with antigen. Stability studies of the ^{64}Cu-minibody showed that after incubation of the protein at either 4°C or 37° for 24–48 h in normal saline/1% HSA, >98% of the radioactivity remained associated with the 80-kDa molecular species, and the labeled protein was >90% immunoreactive (data not shown).

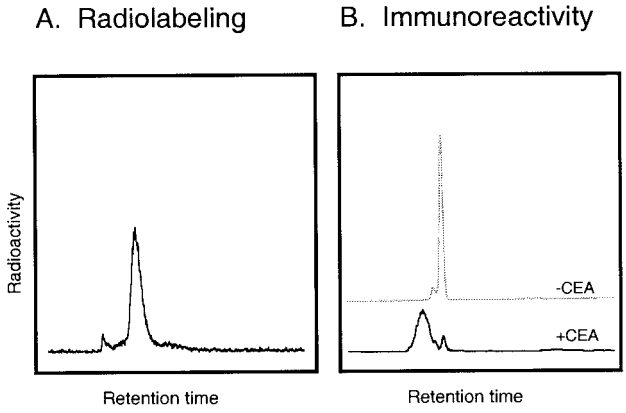

Fig. 2. Size-exclusion HPLC analysis of ^{64}Cu-radiolabeled anti-CEA minibody. (*A*) Analysis and purification of radiolabeled minibody; peak fractions were pooled for animal studies. (*B*) Upper trace, starting sample used for evaluation of immunoreactivity. Lower trace, after incubation with CEA the bulk of the ^{64}Cu-minibody is found in antibody/antigen complexes.

^{64}Cu-Anti-CEA Minibody Localized Rapidly and Specifically to CEA-Positive Xenografts. To evaluate tumor targeting of the ^{64}Cu-minibody, antigen-positive (LS174T colorectal carcinoma) and antigen-negative control (C6 glioma) xenografts were established by s.c. inoculation in athymic mice. MicroPET imaging studies were typically conducted when tumor sizes reached 100–250 mg (approximately 6–8 mm in diameter). In one study, a mouse was injected with 26 μCi of ^{64}Cu-minibody, and a whole-body microPET scan was obtained beginning 5 h after administration. The image in Fig. 3*B* clearly demonstrates high uptake into the positive tumor and low activity in the control tumor. From the three-dimensional reconstruction, 10 planes (of 64 total) were selected in the coronal orientation, encompassing the tumors, and activities were averaged for ROI analysis. Uptake in the LS174T xenograft was 17.7%ID/g, compared with the C6 xenograft at 5.2%ID/g. Thus, the positive tumor/control tumor uptake ratio for the ^{64}Cu anti-CEA minibody was 3.4:1, demonstrating specificity. In fact, control tumor activity was comparable to soft tissue, which gave a background activity of

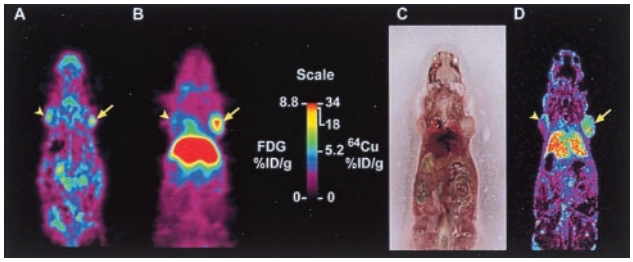

Fig. 3. (*A*) MicroPET scan of mouse administered 200 μCi ^{18}F-FDG and scanned 1 h after injection. The mouse carried a C6 glioma xenograft on the left shoulder and an LS174T xenograft on the right shoulder (arrows). (*B*) MicroPET scan of the same mouse injected with 26 μCi ^{64}Cu-anti-CEA minibody and imaged at 5 h with the highest retention in the LS174T tumor (arrow) and liver and lower retention in the control tumor (arrowhead). (*C*) Mouse was killed for whole-body autoradiography, and an anatomic photograph was taken at the time of sectioning. (*D*) Digital autoradiograph of adjacent section.

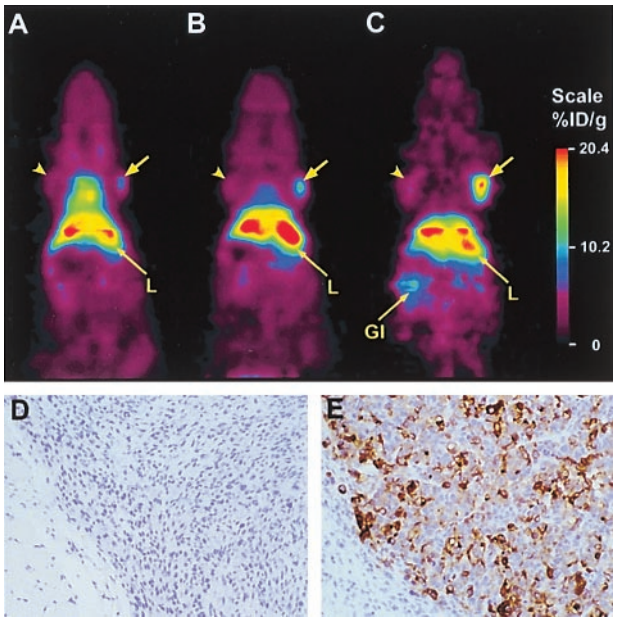

Fig. 4. Serial microPET scans of a mouse bearing bilateral C6 (arrowhead) and LS174T (arrow) xenografts, injected with ^{64}Cu minibody and imaged at 2 h (*A*), 6 h (*B*), and 24 h (*C*). After the final scan, tumors were excised and subjected to immunohistochemical staining by using anti-CEA cT84.66 as the primary antibody. Photomicrographs of C6 (*D*) and LS174T (*E*) xenografts.

5.1%ID/g and a tumor/background ratio of 3.5:1. Also apparent was high liver activity (31.2%ID/g); it appeared that the rapid clearance observed for radiometal chelate-labeled minibodies was via the hepatobiliary system, where the radiolabeled protein or its labeled metabolite remained localized.

MicroPET Signal Corresponded to Antibody Activity Localized at CEA-Positive Tumor. To demonstrate that the uptake detected by microPET scanning of a living animal corresponded to radiolabeled anti-CEA minibody that had localized appropriately to an antigen-positive tumor after the microPET scan, the mouse was immediately killed and subjected to digital whole-body autoradiography. Comparison of the microPET image encompassing the C6 and LS174T xenografts (Fig. 3*B*) and a corresponding DWBA section (Fig. 3*D*) clearly demonstrates that the region of high uptake observed in the scan correlates with autoradiographically detected tumor-associated radioactivity. Furthermore, an ^{18}F-FDG microPET scan of the same animal, performed before the engineered antibody scan, allowed visualization of both tumors (Fig. 3*A*). In this instance, the LS174T xenograft demonstrated higher metabolic activity than the C6 glioma (1.5-fold higher FDG activity); such variations in physiology are not uncommon in tumor xenograft models.

Serial MicroPET Imaging Demonstrated Increasing Tumor/Background Ratios. Imaging by microPET allowed evaluation of tracer localization and distribution over time in the same animal. A mouse was injected with 38 μCi of ^{64}Cu-minibody and serial scans acquired beginning at 2 h, 6 h, and 24 h after administration. Fig. 4*A* (2 h) primarily revealed blood pool and general tissue distribution, and activity was also apparent in the LS174T xenograft (72 mg). At 6 h (Fig. 4*B*), the highest signal appeared in the positive tumor and liver, and by 24 h an intense signal was present in the LS174T tumor, with continued high hepatic activity (Fig. 4*C*). Low activity was present in the control C6 xenograft (155 mg) and was also visible in the kidney. Direct quantitation from the microPET scan demonstrated that ^{64}Cu-minibody activity reached levels above 20%ID/g in the LS174T xenograft at 24 h. The tumor/soft tissue background ratio for this mouse increased from 1.5:1 (2 h) to 3.1:1 (6 h) to 6.1:1 (24 h). Immunohistochemical staining of tissues removed at the end of the scan by using the parental cT84.66 anti-CEA antibody confirmed high expression of CEA in the LS174T xenograft (Fig. 4*E*) and its absence in the C6 tumor (Fig. 4*D*), liver, and kidney (not shown).

Table 1. Uptake of ^{64}Cu-DOTA-minibody as measured by microPET imaging

Tissue	5 h (n = 4)	12 h (n = 4)
LS174T tumor	17.91 (3.66)	15.53 (5.65)
C6 tumor	6.02 (1.04)	6.26 (0.97)
Liver	32.36 (7.81)	21.61 (4.71)
Soft tissue	5.12 (0.58)	3.68 (0.92)

Uptake is expressed as %ID/g. The column labeled ''5 h'' includes mice scanned beginning 4, 5, or 6 h after injection. Results are presented as mean (SE).

MicroPET Imaging Was Successful Under a Variety of Conditions. Xenograft imaging was successful in 11 of 11 animals bearing LS174T tumors of different sizes (ranging from 27 to 395 mg). Administered activities ranged from 26–88 μCi of ^{64}Cu anti-CEA minibody (12–20 μg protein/mouse), and imaging time points spanned 2–24 h after injection. Quantitation of microPET scans showed that LS174T CEA-positive tumor uptakes averaged 17.91%ID/g ($\pm$3.66; n = 4) at 5 h and remained at 15.53%ID/g ($\pm$5.65, n = 4) at 12 h (Table 1). Control tumor activities were 6.02%ID/g ($\pm$1.04) and 6.26%ID/g ($\pm$0.97) at 5 and 12 h, respectively (Table 1). Target/background ratios determined at 5 and 12 h timepoints are summarized in Table 2. Statistical analysis (t test) demonstrated that the signal from LS174T xenografts could be reliably distinguished from the antigen-negative C6 gliomas ($P < 0.05$).

Discussion

A ^{64}Cu-labeled genetically engineered antibody fragment has been developed and shown to be an effective tracer for antigen-based tumor imaging by using a dedicated small-animal microPET scanner. Detection was rapid and sensitive and allowed quantitation of uptake in living animals. The tracer was based on an anti-CEA minibody, a genetically engineered fragment that previously demonstrated rapid high-level tumor uptake coupled with fast clearance from the circulation in preclinical studies of radioiodinated protein (12). Radiolabeling with copper-64 through a DOTA-moiety conjugated to the GS18 minibody was accomplished without loss of immunoreactivity. CEA-positive xenografts could be detected by microPET within a few hours after injection of tracer. Target/background ratios and the resultant quality of the images improved when the imaging time was extended to 12–24 h after injection. Resolution and sensitivity of the microPET instrument were demonstrated through detection of a 27-mg ($\approx$3–4 mm diameter) tumor after localization of the ^{64}Cu-labeled anti-CEA minibody. Uptake levels reached 15–18%ID/g for the ^{64}Cu-minibody, as compared with

Table 2. Target/background ratios were calculated for individual mice from microPET images and then averaged

Comparison	5 h (n = 4)	12 h (n = 4)
Tumor/control tumor	2.98 (0.44)	2.47 (0.89)
Tumor/liver	0.57 (0.18)	0.71 (0.20)
Tumor/soft tissue	3.50 (0.61)	4.13 (0.75)

Results are presented as mean (SE).

3–10%ID/g typically attained in these xenografts by using the tracer FDG (not shown). Comparison with control tumor (6%ID/g) supports antigen binding as the major mechanism of localization. However, the possibility cannot be excluded that some of the observed early uptake in the LS174T tumor, as compared with C6, is because of nonspecific factors such as high permeability in this xenograft model. For example, Aloj *et al.* recently assessed permeability of ^{18}F-transferrin and ^{14}C-albumin (two proteins with molecular weights similar to that of the minibody) in LS174T, observing 4.8 and 8.2%ID/g, respectively, at 6 h after administration (36). Earlier work from our group showed similar uptake of control ^{111}In-DTPA anti-(P450) intact antibody in LS174T (37). Minibody proteins that bind irrelevant antigens have been constructed and will provide an additional specificity control. Uptake values determined by microPET correlated well with direct counting of tissue samples, consistent with previous results (38). The present work demonstrates the use of microPET scanning as a method of quantitative imaging in living animals, based on antibody/antigen recognition.

Radiolabeled anti-CEA antibodies for imaging cancer have been evaluated in a variety of clinical applications, for example, detection of extrahepatic lesions for diagnosis or during restaging of colorectal carcinomas. This ^{64}Cu anti-CEA minibody has advantages over whole antibodies in current use because of its rapid clearance from the circulation. The minibody also offers advantages over conventional Fab fragments, as it is capable of bivalent binding. However, high retention of activity in the liver would limit use in detection of hepatic lesions. Studies are in progress to develop alternate linker chemistries for attachment of DOTA to antibodies and fragments that would allow metabolism and subsequent clearance of activity (34, 35). Alternately, the anti-CEA minibody can be radiolabeled with iodine-123 (for single-photon imaging) or iodine-124 (for PET); in animal studies of ^{123}I-minibody, liver and kidney activity was shown to decline rapidly because of dehalogenation (12).

Another increasingly important application for radioimmunoimaging is in conjunction with radioimmunotherapeutic approaches for cancer. Quantitative imaging before therapy allows evaluation of tumor targeting and patient-specific dose estimation. Current single-photon approaches with planar or single-photon emission computerized tomography, however, have lower spatial resolution and are less quantitative than PET for mapping out the normal organ and tumor doses. Use of a ^{64}Cu-labeled antibody or fragment for PET imaging would provide a quantitative high-resolution approach for determining antibody localization and estimation of radiation doses to tumor and normal tissue. The therapeutic radionuclide could be either copper-64 itself or copper-67, both of which have been shown to be suitable agents for radioimmunotherapy (20, 24, 39).

Finally, the present approach can readily be extended to other tumor-specific antibodies. Hybridoma-derived antibodies can be cloned and reformatted as scFv-C_H3 fusion proteins and are expected to have similar pharmacokinetic properties, i.e., sufficient circulating activity in the first few hours to allow adequate tumor localization but overall rapid clearance kinetics. A large repertoire of monoclonal antibodies with well-characterized specificities is currently in use. Rapid advances in genomics, proteomics, and phage display are expected to yield new information that will provide starting points for producing engineered minibodies with more favorable *in vivo* properties as molecular imaging probes and as potential therapeutics. Thus the detection of positron-emitter labeled recombinant fragments by microPET has potential for broad application in many areas of biological investigation. The present study also sets the foundation for application of ^{64}Cu-anti-CEA-minibody in human studies in addition or as an alternate to FDG in the imaging of CEA positive tumors with clinical PET scanners. The combined high sensitivity of PET with the rapid targeting and high specificity of ^{64}Cu-anti-CEA-minibody should lead to improvement in imaging assays for the management of CEA-expressing tumors.

We gratefully acknowledge the expert assistance of Louise Shively, Cheryl Clark, Chia-Wei Cheung, Millie Martinez, Randall Woo, Jianyi Wang, Alison Green, and Xiaojun Sun. We are grateful to Dr. Simon Cherry and colleagues for ongoing development and support of the microPET. We thank Drs. Sharon Wilczynski and Yan Yu Sun of the City of Hope Cancer Center Anatomic Pathology Core Facility [National Institutes of Health (NIH) CA 33572] for performing the immunohistochemical analysis. Work at the City of Hope was funded through NIH grant CA 43904 and Department of Defense grant DAMD17–00-1–0150. A.M.W., L.E.W., J.E.S., A.A.R., and J.Y.C.W. are members of the City of Hope Cancer Center (NIH CA 33572). Support for studies at UCLA was provided by the Departments of Energy (DE-FC03-ER60615) and Defense (DAMD17–00-1–0150), and work at the Mallinckrodt Institute of Radiology was funded by NIH Research Resource grant CA 86307. The authors also thank Drs. Patricia E. Phelps and Michael R. Lewis for their key roles in the initiation of these collaborations.

1. Goldenberg, D. M. & Larson, S. M. (1992) *J. Nucl. Med.* **33,** 803–814.
2. Goldenberg, D. M. (1997) *Cancer Suppl.* **80,** 2431–2435.
3. Moffat, F. L., Jr., Gulec, S. A., Serafini, A. N., Sfakianakis, G. N., Pop, R., Robinson, D. S., Franceschi, D., Boggs, J. & Livingstone, A. S. (1999) *Cancer Invest.* **17,** 322–334.
4. Buchegger, F., Haskell, C. M., Schreyer, M., Scazziga, B. R., Randin, S., Carrel, S. & Mach, J. P. (1983) *J. Exp. Med.* **158,** 413–427.
5. Behr, T., Becker, W., Hannappel, E., Goldenberg, D. M. & Wolf, F. (1995) *Cancer Res.* **55,** S5777–S5785.
6. Neumaier, M., Shively, L., Chen, F. S., Gaida, F. J., Ilgen, C., Paxton, R. J., Shively, J. E. & Riggs, A. D. (1990) *Canc. Res.* **50,** 2128–2134.
7. Shively, J. E. & Beatty, J. D. (1985) *Crit. Rev. Oncol. Hematol.* **2,** 355–399.
8. Goldenberg, D. M., DeLand, F., Kim, E., Bennett, S., Primus, F. J., van Nagell, J. R., Estes, N., DeSimone, P. & Rayburn, P. (1978) *N. Engl. J. Med.* **298,** 1384–1388.
9. Beatty, J. D., Duda, R. B., Williams, L. E., Sheibani, K., Paxton, R. J., Beatty, B. G., Philben, V. J., Werner, J. L., Shively, J. E., *et al.* (1986) *Cancer Res.* **46,** 6494–6502.
10. Wu, A. M., Chen, W., Raubitschek, A. A., Williams, L. E., Fischer, R., Hu, S., Odom-Maryon, T., Wong, J. Y. C. & Shively, J. E. (1996) *Immunotechnology* **2,** 21–36.
11. Wu, A. M., Williams, L. E., Zieran, L., Padma, A., Sherman, M. A., Bebb, G. G., Odom-Maryon, T., Wong, J. Y. C., Shively, J. E., *et al.* (1999) *Tumor Targeting* **4,** 47–58.
12. Hu, S., Shively, L., Raubitschek, A. A., Sherman, M., Williams, L. E., Wong, J. Y. C., Shively, J. E. & Wu, A. M. (1996) *Cancer Res.* **56,** 3055–3061.
13. Hoh, C. K., Schiepers, C., Seltzer, M. A., Gambhir, S. S., Silverman, D. H., Czernin, J., Maddahi, J. & Phelps, M. E. (1997) *Semin. Nucl. Med.* **27,** 94–106.
14. Cherry, S. R., Shao, Y., Silverman, R. W., Chatziioannou, A., Meadors, K., Siegel, S. 1., Farquhar, T., Young, J., Jones, W. F., *et al.* (1997) *IEEE Trans. Nucl. Sci.* **44,** 1161–1166.
15. Qi, J., Leahy, R. M., Cherry, S. R., Chatziioannou, A. & Farquhar, T. H. (1998) *Phys. Med. Biol.* **43,** 1001–1013.
16. Bakir, M. A., Eccles, S. A., Babich, J. W., Aftab, N., Styles, J. M., Dean, C. J. & Ott, R. J. (1992) *J. Nucl. Med.* **33,** 2154–2160.
17. Rubin, S. C., Kairemo, K. J. A., Brownell, A.-L., Daghighian, F., Federici, M. G., Pentlow, K. S., Finn, R. D., Lambrecht, R. M., Hoskins, W. J., *et al.* (1993) *Gyn. Oncol.* **48,** 61–67.
18. Wilson, C. B., Snook, D. E., Dhokia, B. D., Watson, I. A., Lammertsma, A. A., Lambrecht, R., Waxman, J., Jones, T. & Epenetos, A. A. (1991) *Int. J. Cancer* **47,** 344–347.
19. Larson, S. M., Pentlow, K. S., Volkow, N. D., Wolf, A. P., Finn, R. D., Lambrecht, R. M., Graham, M. C., Di Resta, G., Bendriem, B., *et al.* (1992) *J. Nucl. Med.* **33,** 2020–2023.
20. Deshpande, S. F., DeNardo, S. J., Meares, C. F., McCall, M. J., Adams, G. P., Moi, M. K. & DeNardo, G. L. (1988) *J. Nucl. Med.* **29,** 217–225.
21. Anderson, C. J., Connett, J. M., Schwarz, S. W., Rocque, P. A., Guo, L. W., Philpott, G. W., Zinn, K. R., Meares, C. F. & Welch, M. J. (1992) *J. Nucl. Med.* **33,** 1685–1691.
22. Philpott, G. W., Schwarz, S. W., Anderson, C. J., Dehdashti, F., Connett, J. M., Zinn, K. R., Meares, C. F., Cutler, P. D., Welch, M. J., *et al.* (1995) *J. Nucl. Med.* **36,** 1818–1824.
23. Anderson, C. J., Schwarz, S. W., Connett, J. M., Cutler, P. D., Guo, L. W., Germain, C. J., Philpott, G. W., Zinn, K. R., Greiner, D. P., *et al.* (1995) *J. Nucl. Med.* **36,** 850–858.

24. Connett, J. M., Anderson, C. J., Guo, L. W., Schwarz, S. W., Zinn, K. R., Rogers, B. E., Siegel, B. A., Philpott, G. W. & Welch, M. J. (1996) *Proc. Natl. Acad. Sci. USA* **93,** 6814–6818.
25. Otsuka, F. L., Welch, M. J., Kilbourn, M. R., Dence, C. S., Dilley, W. G. & Wells, S. A. (1991) *Nucl. Med. Biol.* **7,** 813–816.
26. Garg, P. K., Garg, S. & Zalutsky, M. R. (1991) *Bioconj. Chem.* **2,** 44–49.
27. Choi, C. W., Lang, L., Lee, J. T., Webber, K. O., Yoo, T. M., Chang, H. K., Le, N., Jagoda, E., Paik, C. H., *et al.* (1995) *Cancer Res.* **55,** 5323–5229.
28. Bebbington, C. R., Renner, G., Thomson, S., King, D., Abrams, D. & Yarranton, G. T. (1992) *BioTechnology* **10,** 169–175.
29. Bebbington, C. R. (1991) *Methods Companion Methods Enzymol.* **2,** 136–145.
30. You, Y. H., Hefta, L. J., Yazaki, P. J., Wu, A. M. & Shively, J. E. (1998) *Anticancer Res.* **18,** 3193–3202.
31. Lewis, M. R., Raubitschek, A. A. & Shively, J. E. (1994) *Bioconj. Chem.* **5,** 565–576.
32. McCarthy, D. W., Shefer, R. E., Klinkowstein, R. E., Bass, L. A., Margeneau, W. H., Cutler, C. S., Anderson, C. J. & Welch, M. J. (1997) *Nucl. Med. Biol.* **24,** 35–43.
33. McCarthy, D. W., Bass, L. A., Cutler, P. D., Shefer, R. E., Klinkowstein, R. E., Herrero, P., Lewis, J. S., Cutler, C. S., Anderson, C. J., *et al*. (1999) *Nucl. Med. Biol.* **26,** 351–358.
34. Pileri, S. A., Roncador, G., Ceccarelli, C., Piccioli, M., Briskomatis, A., Sabattini, E., Ascani, S., Santini, D. & Piccaluga, P. P. (1997) *J. Pathol.* **183,** 116–123.
35. Gambhir, S. S., Barrio, J. R., Phelps, M. E., Iyer, M., Namavari, M., Satyamurthy, N., Wu, L., Green, L. A., Bauer, E., *et al*. (1999) *Proc. Natl. Acad. Sci. USA* **96,** 2333–2338.
36. Aloj, L., Jagoda, E., Lang, L., Caraco, C., Neumann, R. D., Sung, C. & Eckelmen, W. C. (1999) *J. Nucl. Med.* **40**.
37. Jakowatz, J. G., Beatty, B. G., Vlahos, W. G., Porudominsky, D., Philben, V. J., Williams, L. E., Paxton, R. J., Shively, J. E. & Beatty, J. D. (1985) *Cancer Res.* **45,** 5700–5706.
38. MacLaren, D. C., Gambhir, S. S., Satyamurthy, N., Barrio, J. R., Sharfstein, S., Toyokuni, T., Wu, L., Berk, A. J., Cherry, S. R., *et al*. (1999) *Gene Ther.* **6,** 785–791.
39. Apelgot, S., Coppey, J., Gaudemer, A., Grisvard, J., Guille, E., Sasaki, I. & Sissoeff, I. (1989) *Int. J. Radiat. Biol.* **55,** 365–384.